

SOA-NOLM Based Device for Increasing the Extinction Ratio and Attenuation of Unmodulated Content of an Optical Carrier

Beatriz A. Ribeiro, Fátima L. D. Soares, Ricardo M. Ribeiro and Vinicius N. H. Silva

Abstract— This paper describes the experimental demonstration of a fibre-optic device able to attenuate the unmodulated content and simultaneously enhances the extinction ratio (ER) of an optical carrier. The main aim is to show the proof-of-concept. The active device configuration is based on a Nonlinear Optical Loop Mirror (NOLM) incorporating a Semiconductor Optical Amplifier (SOA) as a compact non-linear element. Results show a 14.6 dB increase of extinction ratio (ER). The unmodulated optical offset could be reduced by 11.2 dB.

Keywords—*Suppression of Optical Carrier, Semiconductor Optical Amplifier, NOLM, Extinction Ratio.*

I. INTRODUCTION

An analogue or digital optically modulated signal may be accompanied with an unmodulated component, i.e. an optical offset or background with almost the same wavelength of the modulated one [1-3].

A typical scenario is a direct analogue modulation of a laser diode where the applied current bias and the small-signal modulating produce an optical offset and a low extinction-ratio (ER), respectively.

By assuming the presence of an unmodulated optical component in the end of a fibre-optic link, the following drawbacks are expected.

Usually, any photo-receiver encompasses a photo-diode followed by a transimpedance pre-amplifier (TIA) and sometimes a post-amplifier with automatic gain control (AGC) [4]. Depending on the optical offset level compared with the modulated component amplitude may be still possible to perform the photo-detection without saturation or even without generation of non-linearities from the photo-diode/amplifier. Therefore, the electrical DC component may be electronically suppressed by using a capacitive coupling circuit, e.g. bias-T or an AC-coupled oscilloscope. However, when the optical offset is excessive or much larger than the modulated component level, occur the saturation of the photo-diode and turn to be no longer possible to electronically suppress the offset. Even the photo-diode is not saturated it may limit the gain setting of the pre-amplifier in order to avoid saturation. An optical pre-amplifier preceding the photo-receiver also amplifies the optical offset thus also contributing to the saturation. By using an optical attenuator, the optical offset level can be reduced, but the modulated component is reduced in the same proportion.

Larger unmodulated optical carrier results in stronger shot-noise (SN) generated in the photo-detection process because the SN is proportional to the mean detected current $\langle I_D \rangle$ that in turn is proportional to the mean optical power.

Therefore, the optical offset limits the sensitivity of the photo-receiver at least in three ways: saturating the photo-diode, limiting the pre-amplifier gain and increasing the SN.

In all-optical signal processing [5-8] many functions are carried out in the optical domain without digitisation before the optical to electrical conversion. An optical offset may be undesirable in all-optical processing devices mainly in those using cascaded circuits.

It was already shown the suppression of the optical offset (or CW background) accompanying optical pulses representing digital signals by using the Dispersion-Imbalanced Nonlinear Optical Loop Mirror (DI-NOLM) configuration working in the time-domain [2,9]. The use of NOLMs and similar circuits generally require long length of optical fibres and/or high peak power. The unmodulated optical carrier may be also suppressed by using a suitable hyperfine filter [1].

It was early reported by our group, the proposal, design and numerical simulations of a Sagnac fibre-loop incorporating a SOA as an all-optical device intended to reduce or suppress the optical offset [10]. None experiments were presented at that time.

This paper describes the experimental demonstration of the proposed all-optical device [10] able to reduce or even to suppress the unmodulated component of an optical carrier whereas it can enhance the ER. In order to show the proof-of-concept, the experiments were constrained by using 200 MHz sinewave signal superposed with an optical offset. Furthermore, in section IV the application scenario of the presented device is further detailed.

II. THE EXPERIMENTAL OPTICAL CIRCUIT AND PRINCIPLE OF OPERATION

Figure 1 schematically shows the optical circuit of the proposed device as was built in the laboratory. The circuit consists of a Sagnac fibre-loop interferometer incorporating an asymmetrically inserted SOA as the nonlinear element also known in the literature as SOA-NOLM configuration [11,12].

Beatriz A. Ribeiro, Fátima L. D. Soares, Ricardo M. Ribeiro and Vinicius N. H. Silva, Departamento de Engenharia de Telecomunicações, Universidade Federal Fluminense, UFF 24.210-240 - Niterói, RJ – Brasil, beatrizar@id.uff.br

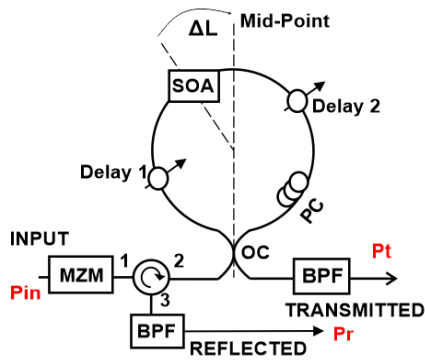


Fig. 1. The schematic drawn of the SOA-NOLM configuration as a device intended to be simultaneously an optical offset attenuator and ER enhancer.

The input optical signal P_{in} (power) was generated by using a Mach-Zehnder electro-optic modulator biased at the quadrature. Therefore, the P_{in} was comprised by a modulated superposed with an unmodulated component (offset) as is shown in Fig. 2a. The P_{in} was launched in the port 1 of an optical circulator thus exiting in the port 2. The latter was connected to a fibre-optic splitter (50/50 coupling factor at 1550 nm) used to build a Sagnac interferometer. A polarisation controller (PC) from ProtoDel was inserted in order to optically biasing the interferometer. The fibre-optic delays were inserted to create the needed asymmetry (ΔL) of the SOA position in the loop by assuming the midpoint as the reference.

The inserted SOA in the loop was a 1550 nm non-linear model from Kamelian (UK) presenting 1 mm length, 25 ps gain recovery time and 12 dB maximum optical amplification gain.

The P_{in} is launched in the Sagnac loop and the coupler split the optical signal in two copies of approximately the same power, i.e. the clockwise (cw) and counter-clockwise (ccw) components that propagates in opposite direction around the loop. The cw and ccw components interfere at the coupler leading to P_r and P_t optical power exiting the “reflective” and “transmitter” output of the Sagnac interferometer, respectively. The PC allows the control of the power balance between the reflected (P_r) and the transmitted (P_t) signals. For instance, the loop may be adjusted to operate in quadrature ($P_t = P_r$), as a loop mirror ($P_t = 0$), etc. The optical circulator recovers the P_r power since it outputs through the port 3. The P_t component is the “output” signal of the device that traverses a C-band tuneable band-pass filter (BPF) from Lightwave 2020 before reaches the 1.2 GHz bandwidth InGaAs DET01CFC biased photo-detector (Thorlabs). The BPF was used to reduce the ASE noise generated by the SOA. The photo-detector was connected to a 352A digital oscilloscope (LeCroy).

The operation of the circuit is primarily based on the strong resonant optical nonlinearity presented by the SOA through the self-phase modulation (SPM) mechanism combined with the interference provided by the Sagnac loop. The asymmetric placement ΔL of SOA relative to the fibre-loop midpoint is needed to open an “SPM-based switching window” thus leading the device to switch out the launched signals [11].

The continuous-wave component of the launched signal is not affected by SPM leading to be not switched out as the power is increased, i.e. it is mostly reflected. However, the modulated component may be partially or totally switched out

to the transmitter port of the interferometer. In a simple statement, the “unmodulated optical offset” is rather reflected whereas the “modulated optical component” is rather transmitted (or switched).

As a result of some preliminary experimental trials performed to reduce as much as possible the unmodulated optical carrier level output, some device settings were found to be: $I_{BIAS}(SOA) = 244$ mA, optical delays of 13ns/17ns and 1550.5 nm wavelength.

III. RESULTS AND DISCUSSIONS

The Extinction Ratio (ER) is determined from the equation 1:

$$ER = \frac{AC + Offset}{Offset} = 1 + \frac{AC}{Offset} \quad (1)$$

AC is the modulated component level and offset is the unmodulated component level. It can be seen from Figure 2a the input waveform with a large unmodulated component (offset). Figure 2b shows the corresponding Fast-Fourier Transform (FFT) signal.

The modulated component was a 200 MHz sinewave with $P_{modulated} = 9.4$ mV modulated amplitude. The unmodulated component presented $P_{offset} = 17.3$ mV level. Figure 2b shows that the input signal presents harmonic distortion characterised by the $P_{fundamental}/P_{2nd-harmonic} = -50 - (-90) = 40$ dB ratio. The ER of the input signal was $ER_{input} = 1 + 9.4/17.3 = 1.54 (= 1.87$ dB).

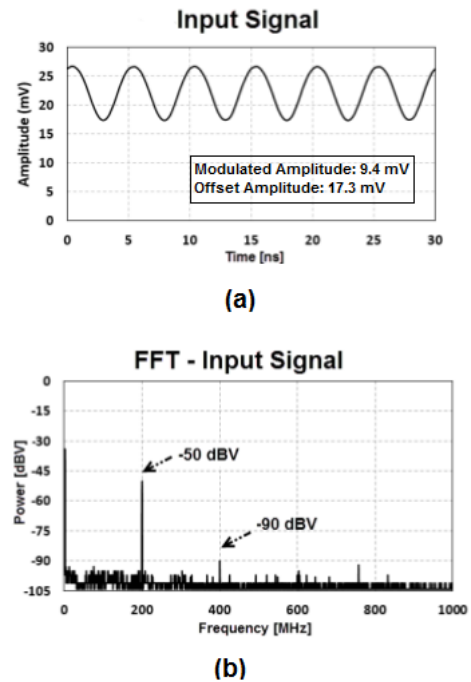


Fig. 2. (a) The input signal consisting of a 200MHz frequency modulated single-tone (sinewave) superposed with an unmodulated component. (b) The FFT of the input signal.

Figure 3a shows the two-components (modulated component + unmodulated offset) of the output waveform. Figure 3b shows the corresponding FFT signal.

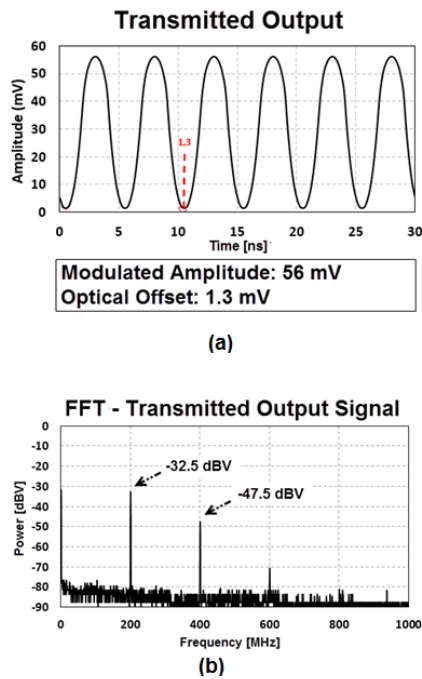


Fig. 3. (a) The transmitted output signal waveform in the time-domain. (b) The FFT from the transmitted output signal waveform.

The modulated component was a 200 MHz somewhat distorted sinewave with $P_{\text{modulated}} = 56 \text{ mV}$ modulated amplitude. The offset presented $P_{\text{offset}} = 1.3 \text{ mV}$ level. The ER from the transmitted signal was $ER_{\text{transmitted}} = 1 + 56/1.3 = 44.07$ ($= 16.44 \text{ dB}$).

By comparing the input and output signals as shown in Figs. 2a and 3a, it can be seen that the ER has increased of $16.44 - 1.87 = 14.57 \text{ dB}$. Likewise, the modulated component was amplified by $56 \text{ mV}/9.4 \text{ mV} = + 7.8 \text{ dB}$ while the unmodulated level was attenuated by $1.3 \text{ mV}/17.3 \text{ mV} = - 11.2 \text{ dB}$. From Figure 3b, it can be seen that the fundamental and second harmonic components are $\sim 15 \text{ dB}$ apart that should be compared with the initial 40 dB . It was verified that with variations of $\pm 5\%$ around 200 MHz , there was little impact on the quality of the transmitted signal, presenting little distortion and change in the spectral content.

Figure 4a shows the two-components reflected waveform. Figure 4b shows the FFT corresponding to the reflected signal. As can be seen from Figure 4a, the unmodulated reflected signal by the loop is a “complement” of the transmitted signal. It features a modulated component and an optical offset level both being optically amplified. The signal as measured from the reflection port is expected in the sense that the unmodulated carrier (Offset) level is almost completely switched to this port. Therefore, the optical offset level of the transmitted signal is quite attenuated whereas the modulated component is amplified after comparison with the input signal. The presence of modulated component in the reflected arm shows that the not all modulated content is switched to the transmission arm.

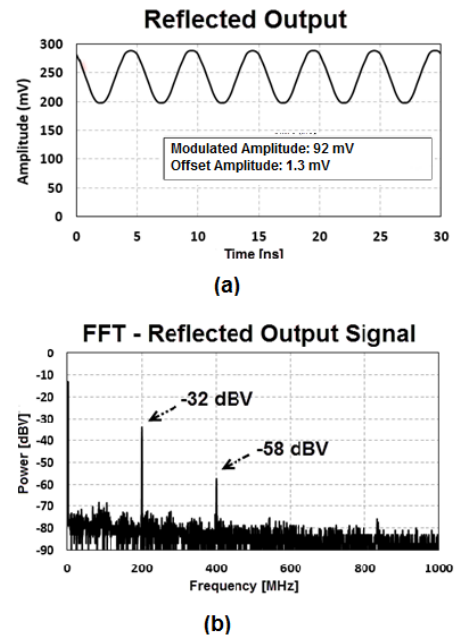


Fig. 4. (a) The reflected output signal waveform in the time-domain. (b) The FFT from the reflected output signal waveform

Tables 1 and 2 quantitatively summarise the experimental results as previously described.

TABLE I. RESULTS FROM THE EXPERIMENT.

SIGNAL COMPONENT	INPUT	OUTPUT (TRANSMITTED)
Modulated	9.4 mV	56 mV
Offset Level	17.3 mV	1.3 mV
Extinction Ratio (ER)	1.87 dB	16.44 dB

TABLE II. THE ER INCREASE AND OPTICAL OFFSET LEVEL SUPPRESSION.

PARAMETER	EXPERIMENTS
ER increase	+ 14.57 dB
Modulated Component Amplification	+ 7.8 dB
Optical Offset Level Suppression	- 11.2 dB

As summarised in Tables 1 and 2, the proposed device in present development stage was able to suppress the optical offset level by 11.2 dB while simultaneously increases the ER by 14.57 dB . Therefore, the device behaves like a “differential optical amplifier” in the sense that it is able to reduce/suppress the unmodulated component level of an optical carrier whereas simultaneously amplifying the modulated one or improving the ER.

However, it was observed an increase of harmonic distortion $P_{\text{fundamental}}/P_{\text{2nd-harmonic}}$ from 40 to 15 dB . In order to suppress or attenuate the output (transmitted) optical offset level, the polarisation bias of the SOA-NOLM was firstly adjusted. Under continuous-wave launch, the fibre-loop must be biased as to be almost 100% reflective. Nevertheless, this

procedure generates a distorted output waveform with small amplification gain when compared with the input signal. The reason is likely to be caused by the operating-point located near the maxima or minima of the Sagnac interferometer transfer function, i.e. far from the quadrature point [10]. Therefore, the optical bias was chosen in a way that a commitment between the offset level attenuation and the distortion strength ($P_{2nd\text{-harmonic}}$) were reached. The BPF filter placed at the output port of the device can reject the most of the ASE noise generated by the SOA. However, the filter cannot remove the ASE from their band-pass that adds noise and may cause further distortions in the output signal.

IV. SUGGESTED APPLICATIONS

The DET01CFC biased photo-detector used in the experiments features 5.5 mW (1550 nm) average optical power saturation. The SOA-NOLM device being presented in this paper may be useful when a 200 MHz bandwidth InGaAs APD with TIA from Esterline CMC Electronics (Canada) model 264-339769-101 is employed as the photo-receiver in a fibre-optic link. The NOLM-SOA device is thought to be placed between an optical fibre link and the photo-receiver composed by an avalanche photodiode (APD) with transimpedance amplifier (TIA). Such APD model is very sensitive but presents only $P_{\text{sat}} = 10 \mu\text{W}$ power saturation, much smaller than the 5.5 mW.

Figure 2a shows an input signal generated in the experiments presenting $V_{\text{OSC}} = 17.3 \text{ mV}$ (seen in the oscilloscope) corresponding to $P_{\text{in}} = 346 \mu\text{W}$ optical offset level and $V_{\text{OSC}} = 9.4 \text{ mV}$ corresponding to $P_{\text{in}} = 188 \mu\text{W}$ optical AC amplitude. The correspondence may be easily calculated from $V_{\text{OSC}} = Z_L R_{\text{sp}} P_{\text{in}}$ where V_{OSC} , $Z_L = 50 \Omega$, $R_{\text{sp}} \approx 1 \text{ mA/mW}$, and P_{in} are the voltage displayed by the oscilloscope, the input impedance, the photo-diode responsivity and the input optical power, respectively. Therefore, the APD would be saturated thus leading the link to out of service. However, after processing the input signal by our device, the output signal is given by the $V_{\text{OSC}} = 1.3 \text{ mV}$ leading to $P_{\text{in}} = 26 \mu\text{W}$ optical offset level and $V_{\text{OSC}} = 56 \text{ mV}$ leading to $P_{\text{in}} = 1120 \mu\text{W}$ optical AC amplitude, as is shown in Fig. 3a. In this stage, it can be still find the APD saturation but the use of an $\sim 20 \text{ dB}$ optical attenuator just before the APD may circumvent the drawback.

Another similar example may be depicted by the use of the 430C APD model (Thorlabs) up to 400 MHz bandwidth that presents $P_{\text{sat}} = 22\text{-}110 \mu\text{W}$ saturation power range. The APD + TIA models AD14109A (Anritsu) and KPDXA10C (Kyosemi), both for 10 Gbps, present $316 \mu\text{W}$ and $100 \mu\text{W}$ optical overload, respectively. The effective responsivity $R_{\text{eff}} = MR_{\text{sp}}$, where $M = 10$ typically for InGaAs APDs at small optical signals, decreases as P_{in} is increased. Therefore, the sensitivity of APDs is reduced even their saturation is not reached yet. At least, the optical offset level contributes to reduce the M-factor and then the sensitivity of an APD-based photo-receiver.

An additional application for the NOLM-SOA device is related to RF signals captured by an antenna. RF signals can modulate a laser diode (LD) or an external modulator. In both cases even using amplification, it is expected a modulation with low ER because the captured RF signal is generally of weak amplitude.

Finally, multimode fibre-optic sensors denoted as “modalmetric” require the launch of unmodulated optical carrier as a probe light and outputs low-frequency/low-amplitude modulated signal due to interference buried in a much higher optical offset power level [3]. The latter is very difficult to suppress out with the aim to increase the photo-detection sensitivity.

V. CONCLUSIONS

Many techniques for suppression of optical carrier in the modulation stage (optical transmitter) have been developed [1,13]. However, the NOLM-SOA device here presented is an alternative technique that uses a relatively simple scheme based on a Sagnac fibre-optic loop incorporating a fast SOA. The device is also useful for direct modulation of laser diodes. It can reduce the optical offset level accompanied by a buried sinewave (single-tone analogue) modulation like an “optical capacitor”. Simultaneously, the device can also enhance the ER. However, the output waveform is somewhat distorted. Further investigations are required in order to reduce the distortions created by our device. At least the SOA-NOLM device may be useful for single-octave (narrow) bandwidth links where the harmonic components may be filtered out in the electrical domain. On the other side, the distortions may be reduced or compensated [14] in broadband systems.

It should be observed from section II that the round-trip time of the Sagnac ring was set at $13 + 17 = 30 \text{ ns}$ that is 6 times larger than the modulation period of 5 ns corresponding to the 200 MHz frequency. The best results were achieved when the Sagnac ring round-trip was adjusted to be an integer number of times larger than the period of the input signal. Such achievement is under investigation and will be reported in future publications.

The use of SOA as the nonlinear optical element allows future miniaturisation and the use of moderate-small optical powers. Eventually, it will lead to devices able to perform also additional functions in a single Photonic Integrated Circuits (PICs) [15].

Further experimental developments toward the distortion reduction, higher frequencies operation, digital optical signal processing is scheduled or in progress by our team.

REFERENCES

- [1] Xiao, S. & Weiner, A. M. (2005). Optical carrier-suppressed single sideband (O-CS-SSB) modulation using a hyperfine blocking filter based on a virtually imaged phased-array (VIPA). *Photonics Technology Letters, IEEE*, 17(7), 1522-1524.
- [2] Wong, W.S.T; Namiki, S.; Margalit, M.; Haus, H.A. & Ippen, E.P. (1997). Self-switching of optical pulses in dispersion-imbalance nonlinear loop mirrors. *Optics Letters*, 22(15), 1150-1152.
- [3] Ribeiro, R.M.; Balod, Y.C.; Barbero, A.P.; de Carvalho, M.B. & dos Santos, P.A. Monitoramento da Integridade Física de Cabos Ópticos de Telecomunicações Usando um Sistema Modalétrico no Domínio do Tempo (in Portuguese). Proceedings of the XXVI Simpósio Brasileiro de Telecomunicações, September 2-5, Rio de Janeiro, RJ, Brasil.
- [4] Shukla, A.; Gamad, R. & Raikwar, R. (2013). Design of a CMOS Optical Receiver Front-End Using $0.18 \mu\text{m}$ Technology. *Wireless Engineering and Technology*, 4(1), 46-53.
- [5] Abdollahi, S. (2012). Fully-photonic digital radio over fibre for future super-broadband access network applications (PhD Thesis). Dept. Electronic and Computer Engineering, Brunel University London.

- [6] Willner, A.E.; Khalegui, S.; Chitgarha, M.R. & Yilmaz, O.F. (2014). All-Optical Signal Processing. *Journal of Lightwave Technology*, 32(4), 660-680.
- [7] Khodashenas, P.S. et al (2016). Benefit Evaluation of All-Optical Subchannel Add-Drop in Flexible Optical Networks. *IEEE Photonics Journal*, 8(2), 0601708, 9 pp.
- [8] Guan, P. et al (2016). All-Optical Ultra-High-Speed OFDM to Nyquist-WDM Conversion Based on Complete Optical Fourier Transformation. *Journal of Lightwave Technology*, 34(2), 626-632.
- [9] Wong, W. S. et al. (1998). In-band amplified spontaneous emission noise filtering with a dispersion-imbalanced nonlinear loop mirror. *Journal of Lightwave Technology*, 16(10), 1768-1772.
- [10] Ribeiro, R.M.; Silva, V.N.; Barbero, A.P.; Lucarz, F. & Fracasso, B. (2014, July). Numerical analysis of Sagnac loop incorporating a semiconductor optical amplifier to suppress the unmodulated optical carrier in the time domain. 16th IEEE International Conference on Transparent Optical Networks (ICTON 2014), Graz, Austria, 1-4.
- [11] M. Eiselt, W. Pieper, H. G. Weber, SLALOM: semiconductor laser amplifier in a loop mirror, *J. Lightwave Technol.* 13 (10) (1995) 2099-2112.
- [12] Roncin, Vincent, et al. "SOA-NOLM in Reflective Configuration for Optical Regeneration in High Bit Rate Transmission Systems." arXiv preprint arXiv:1405.2772 (2014).
- [13] Htet, S.N.M. (2014). Generation of Optical Carrier Suppressed Signal for Radio-over-Fiber (RoF) System Using Dual-Drive Mach-Zehnder Modulator. *International Journal of Scientific and Research Publications*, 4(9), 1-7.
- [14] Cox, C.H. (2006). *Analog optical links: theory and practice*. Cambridge University Press.
- [15] Cotter, D. et al (1999). Nonlinear optics for high-speed digital information processing. *Science*, 286(5444), 1523-1528.